Chemicals from biomass: Etherification of 5-hydroxymethyl-2-furfural (HMF) into 5,5′(oxy-bis(methylene))bis-2-furfural (OBMF) with solid catalysts

O. Casanova, S. Iborra, A. Corma *

Instituto de Tecnología Química (UPV-CSIC), Avda dels Tarongers s/n, Universitat Politècnica de València, 46022 Valencia, Spain

ABSTRACT

Starting from 5-hydroxymethyl-2-furaldehyde (HMF), it has been possible to produce 5,5′-oxy(bismethylene)-2-furaldehyde (OBMF), which is an interesting prepolymer and antiviral precursor, using Lewis and Brönsted solid acid catalysts. Structured micro- and mesoporous aluminosilicates are active and selective, but Al-MCM-41 displays the best performance owing to smaller diffusion constraints. The yield obtained is higher than with homogeneous acid catalysts. Metal-substituted zeolites and mesoporous materials bearing Lewis acidity are also active and selective catalysts for the above reaction.

© 2010 Elsevier Inc. All rights reserved.

1. Introduction

The synthesis of fuels and chemicals from biomass makes an emphasis on the necessity to develop environmentally sustainable processes. Since sugars are abundant in nature, it is not surprising that one of the foremost target reactions has been the transformation of sugars into their immediate dehydrated derivative, i.e. 5-hydroxymethyl-2-furfural (HMF) and furfural from hexoses and pentoses, respectively [1,2].

The synthesis of an HMF derivative, such as 5,5′-oxy(bis-methylene)-2-furaldehyde (OBMF), is of much interest for the preparation of some imine-based polymers. For instance, the resulting polymer from the reaction between OBMF and 1,4-diaminobenzene exhibits a high glass transition temperature (300 °C) and high thermal and electrical conductivity [2]. A second important application of OBMF is for the preparation of hepatitis antiviral precursors. This is done by reacting OBMF with 4-amino-pyridine in presence of para-toluenesulphonic acid (pTSA) followed by its reduction with KBH$_4$ [3].

For the synthesis of OBMF, two different routes are found in the literature: (a) the etherification of two HMF molecules catalysed by homogeneous organic acids (e.g. pTSA) using organic solvents (e.g. toluene) to obtain 72 mol% yield [4–6]; (b) Williamson reaction between HMF and 5-chloro-methyl-2-furfural in presence of an excess of base [3]. These two routes are shown in Scheme 1.

When homogeneous acids and bases are used for the conventional synthesis of OBMF, large amounts of residues are generated.

Moreover, in the preparation of OBMF with pTSA using toluene as a solvent, alkylation by-products between the reactant and the solvent are also formed. With the aim of improving the synthesis of OBMF, solid acids have been used. In this sense, it is worth noting the use of alumina [7], silico-aluminates [8], alumino-phosphates [9] and Nafion and Amberlist resins [10–14] to prepare symmetrical ethers. The latter ion-exchange resins are used industrially to synthesize ethers. However, the main disadvantage is their relatively low thermal stability, specially when the catalyst needs to be regenerated.

In order to overcome this limitation, we have thought on using zeolites and mesoporous aluminosilicates with Brönsted and Lewis acid sites. Indeed, the possibilities to modulate acidity and adsorption properties and pore dimensions and topology, together with their well-known thermal stability of the above materials, may offer further possibilities for designing a more efficient environmentally friendly process for the production of OBMF. This should be possible taking into account the work already done regarding the synthesis of ethers using beta and MCM-41 catalysts [15–20].

In this work, we will present a study on the synthesis of OBMF from HMF under mild reaction conditions, using zeolitic and mesoporous catalysts containing framework Brönsted and Lewis acid sites, with yields above 99%.
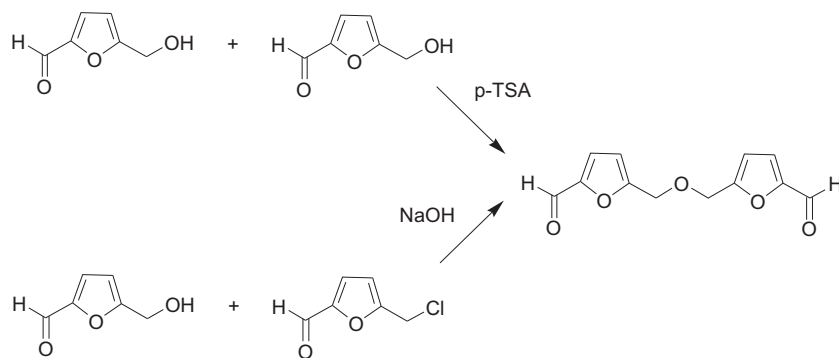
2. Experimental

2.1. Reactants

All the reactants used in this work were purchased from Aldrich unless indicated otherwise: 5-hydroxymethyl-2-furfural (99.8%),

Scheme 1. Synthetic routes of OBMF.

furfural (99%), trifluorotoluene (TFT) (98%, ABCR), anhydrous toluene (99.9%), mesithylene (98%), durene (99%), 4-chlorotoluene (98%), nitrobenzene (99.9%) and para-toluenesulphonic acid (99.8%).

2.2. Catalysts preparation and characterization

H-Mordenite-12.5 (CBV-20A) and *H-Al-Beta 12.5* (CP 811) were purchased from PQ ZEOLITES B.V. and before use, they were calcined at 580 °C for 3 h. The following catalysts were prepared according to the literature: *H-Al-Beta-F 12.5-100* [21], *Nano-H-Al-Beta 19* [22], *Al-MCM-41 12.5* [23], *Sn-Beta* [24], *Zr-Beta* [25], *Nb-Beta, Ta-Beta* [26], *Sn-MCM-41* [27], *Zr-MCM-41, Si-Beta* [28,29] and *Si-MCM-41* [30].

Crystallinity and phase identification of the materials were determined by powder X-ray diffraction (XRD) in a Philips X'Pert MPD diffractometer equipped with a PW3050 goniometer (Cu Kα radiation, graphite monochromator) provided with a variable divergence slit. Infrared (IR) experiments with adsorption of pyridine were performed in a Nicolet 710 FTIR spectrometer using vacuum cells. Wafers of 10 mg cm^{-2} were degassed overnight under vacuum (10^{-4} to 10^{-5} Pa) at 400 °C. The spectra were recorded, then pyridine was admitted and, after equilibration, the samples were outgassed for 1 h at increasing temperatures (150/250/350 °C). After each desorption step, the spectrum was recorded at room temperature and the background subtracted. IR spectra were performed using a Nicolet 750 spectrophotometer. Hence, following the above procedure, the acidity of the catalysts was determined on the basis of a method already described in the literature [31]. The metal content of the calcined samples was determined by atomic absorption in a Varian SpectrAA-10 Plus, elemental analysis (C, H, N) in a Fisons EA1108CHN-S, and Si was

calculated by difference. Specific surface area was measured by nitrogen and argon adsorption experiments at 77 and 85 K, respectively, using a Micromeritics ASAP 2000 apparatus. Thermogravimetric and differential thermal analyses (TGA-DTA) were performed in a Netzsch STA 409 EP thermal analyser with about 20 mg of sample and a heating rate of 10 °C/min in air flow (6 L/h). Gas chromatography (GC) analyses were performed with a Varian 3300 chromatograph equipped with a flame ionization detector, and the capillary column was TRB-5 (5% crosslinked phenyl-methyl silicone) (sizes 30–0.25–0.25) (Teknokroma). Mass spectra were performed by GC–MS (HP Agilent 5973 with a 6980 mass selective detector). Proton nuclear magnetic resonance (^{1}H NMR) spectra were recorded with a varian Gemini at a frequency of 300 MHz. The main characteristics of the catalysts are summarized in Tables 1 and 2.

2.3. Catalytic experiments

The catalytic reactions were carried out in a three-necked round bottom flask reactor equipped with a magnetic stirrer, immersed in a thermostatic oil bath, fitted with a reflux condenser. Prior to reaction, the catalyst was activated by in situ dehydration of the sample at 200 °C for 2 h under vacuum. As a general procedure, 1 mmol HMF was dissolved in 2.3 mL solvent and loaded into the reactor which contained the catalyst. The mixture was stirred at ca. 1000 rpm, and the progress of the reaction was followed by taking samples at regular periods of time and analysed by GC using nitrobenzene as internal standard. When the reaction was finished, the final product was filtered and the catalyst was washed several times with acetone. After evaporation of the solvent, OBMF was obtained as a solid whose structure was confirmed by ^{1}H NMR and MS spectrometry. The used solid catalyst was continuously washed

Table 1
Characterization of Brönsted acid catalysts.

Catalyst	Si/Al mol ratio	Crystal size (nm)	BET area (m^2/g)	Brönsted acidity[a,b] (μmol py/g)		
				150	250	350
H-Mord 12.5	12.5	50–300	550	67	54	29
H-Al-Beta 12.5	12.5	100–200	730	35	20	7
Nano-H-Al-Beta-F 19	19	20	580	62	52	21
Al-MCM-41 12.5	12.5	–	1100	20	5	4
H-Al-Beta-F 12.5	12.5	1000	470	80	57	18
H-Al-Beta-F 25	25	1220	460	55	44	13
H-Al-Beta-F 50	50	1400	475	33	30	12
H-Al-Beta-F 100	100	2000	470	28	20	9

[a] From extinction coefficients by Emeis [31].
[b] Pyridine (py) desorption at the temperatures indicated in °C.

Table 2
Characterization of Lewis acid catalysts.

Catalyst	Si/Metal mol ratio	BET area (m^2/g)	Lewis acidity (μmol py/g)[a,b]		
			150	250	350
Sn-Beta	130	475	11	0	–
Zr-Beta	130	485	14	0	–
Nb-Beta	90	490	9	0	–
Ta-Beta	90	484	13	0	–
Sn-MCM-41	146	1109	13	6	–
Zr-MCM-41	90	1170	1	0	–

[a] From extinction coefficients by Emeis [31].
[b] Pyridine (py) desorption at the temperatures indicated in °C.

with CH_2Cl_2 using a Sohxlet equipment, and the amount of organic recovered was considered in the mass balance (>98%). The extracted catalyst was calcined at 500 °C for 5 h under air flow and reused for successive runs.

Spectral data of OBMF: (1) ^{1}H NMR (300 MHz, CDCl$_3$, TMS as internal standard): δ 9.64 (s, 2H, 2× CHO), 7.22 (d, J = 3.5 Hz, 2H, 2× C3-H), 6.54 (d, J = 3.6 Hz, 2H, 2× C4-H), 4.64 (s, 4H, 2× CH$_2$). (2) GC–MS data (% relative intensity): M$^+$ 234 (C$_{12}$H$_{10}$O$_5$) (1%), 206 (7%), 177 (1%), 138 (3%), 125 (7%), 123 (8%), 110 (43%), 109 (100%), 96 (2%), 95 (18%), 82 (30%), 81 (99%), 79 (7%), 69 (13%), 68 (5%), 53 (94%), 52 (36%), 51 (31%), 50 (16%), 41 (30%) and 39 (59%).

3. Results and discussion

3.1. Influence of pore topology and chemical composition of solids with Brönsted acid sites for the preparation of OBMF

The formation of symmetrical ethers by condensation of two alcohol molecules is typically catalysed by Brönsted acids. In fact, as referred before, the etherification of HMF using pTSA is one of the best options described for the synthesis of OBMF in homogeneous phase [4]. According to the literature, this reaction was carried out at the reflux temperature of toluene, achieving 81 mol% yield with 90 mol% selectivity to OBMF in 3 h (entry 1, Table 3). With the aim of studying and comparing the behaviour of a heterogeneous catalyst with Brönsted acid sites, a protonated beta zeolite having a Si/Al mol ratio of 12.5 (H-Al-Beta 12.5) was selected. Under the same reaction conditions, the selectivity to OBMF was very low (entry 2, Table 3) due to the formation of alkylation products between HMF and toluene. In order to avoid these secondary reactions, the same catalyst was used under reflux (100 °C) with a solvent which contained a deactivated aromatic ring, such as trifluorotoluene (TFT) (entry 3, Table 3). As can be observed in Table 3, the selectivity was nearly 100 mol% towards OBMF at 81% conversion of HMF which already matches the best results obtained with pTSA. It appears then that TFT is a suitable solvent for the tar-

get reaction and will be the solvent used in subsequent experiments.

To study the effect of the pore structure of the catalyst for a given chemical composition (Si/Al mol ratio 12.5), we performed the reaction with a protonated mordenite (H-Mord 12.5) and a mesoporous material such as Al-MCM-41 (entries 4 and 5, Table 3). As can be observed, in Table 3, H-Mord 12.5 displays the lowest catalytic activity, despite its relatively high Brönsted acidity (see Table 1). This can be attributed to the diffusional constraints of reactants and products and pore blockage due to the adsorption of organic compounds within the monodimensional 12-member ring pores of mordenite. Zeolite H-Al-Beta 12.5 follows mordenite in the order of increasing catalytic activity, being Al-MCM-41 the most active. Moreover, we can observe that the rate of catalyst deactivation follows the order: H-Mord 12.5 > H-Al-Beta 12.5 > Al-MCM-41 12.5 (Fig. 1). Taking into account that the silanol groups do not catalyse the etherification reaction (entry 6, Table 3), the higher activity of Al-MCM-41 with respect to the beta zeolite cannot be justified on the basis of its Brönsted acidity, since this is much lower in the former mesoporous catalyst than for H-Al-Beta 12.5 (Table 1). Therefore, the differences in activity between the zeolite and the mesoporous material could be explained considering that in the case of the tridirectional beta zeolite, there is still some molecular diffusion constraints through the micropores, particularly for the bulky OBMF product.

In order to check this hypothesis, the reaction was carried out using a nanocrystalline zeolite beta with a crystallite size of 20 nm (Nano-H-Al-Beta-F 19) (Table 1 and entry 7 in Table 3). When this result is compared with those obtained using a Beta
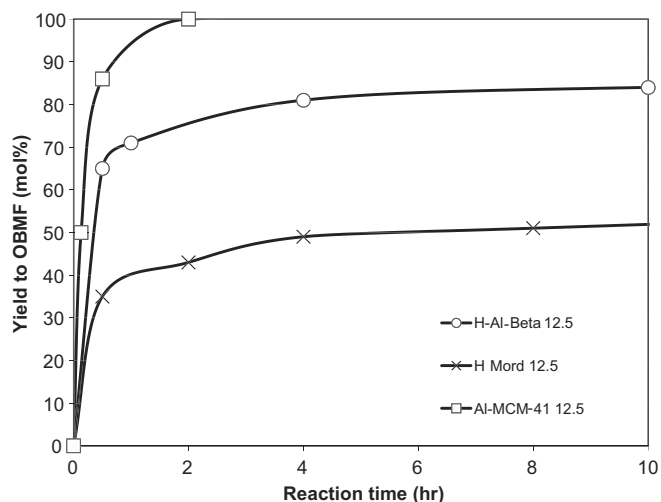

Fig. 1. Kinetics of the yield to OBMF (mol%) obtained for different solid Brönsted acid catalysts, in TFT, at 100 °C and 0.45 M HMF.

Table 3
Etherification of HMF into OBMF with Brönsted acid catalysts.[a]

Entry	Catalyst (solvent)	Initial rate (mmol/h)	t (h)	Conversion (mol%)	Selectivity (mol%)
1	pTSA (toluene)[b]	1.39	3	85	90
2	H-Al-Beta 12.5 (toluene)	1.37	4	96	25
3	H-Al-Beta 12.5 (TFT)	1.30	4	81	>99
4	H-Mord 12.5 (TFT)	0.70	24	58	>99
5	Al-MCM-41 12.5 (TFT)	1.6	2	>99	>99
6	Si-MCM-41 (TFT)	–	24	<1	–
7	Nano-H-Al-Beta-F 19 (TFT)	1.66	4	96	>99

[a] Reaction conditions: 126 mg HMF (1.0 mmol) in 2.3 mL TFT or toluene with 50 mg catalyst was loaded into a three-necked round-bottomed flask. The mixture was heated at 100 °C.
[b] Reaction conditions: a solution of HMF (0.126 g) in toluene (5 mL) containing about 0.2 wt% pTSA was refluxed using a water removal trap.

zeolite sample with crystallite size of 1000 nm (H-Al-Beta-F 12.5), we can see (Fig. 2) that the initial rate is much higher with the nanocrystalline zeolite, which indicates the existence of diffusional constraints. Moreover, the selectivity of H-Al-Beta-F 12.5 is also ca. 99 mol%. The results can be interpreted on the basis of lower diffusional limitations in the nanocrystalline material since this has a much larger external to internal surface ratio than the regular beta zeolite. Then, the results from Fig. 2 indicate that it is possible to achieve high yield of OBMF with a tridirectional pore zeolite such as beta provided that it is synthesized with very small crystallites. At the same time, the results support the hypothesis that the very high yield of OBMF obtained with Al-MCM-41 sample is due to the much larger pore diameter that facilitates the diffusion of reactants and products within the pores. Notice that when Al-MCM-41 was calcined after the reaction and reused under the same conditions, the same results as with fresh Al-MCM-41 12.5 were obtained, confirming catalyst regenerability and reuse.

3.2. Influence of zeolite polarity

The optimization of the activity and selectivity of a catalyst involves not only the optimization of the number and strength of the active sites, but also the adsorption properties. It is known that by increasing the Si/Al ratio of a zeolite, the surface hydrophobicity increases, while the number of acid sites decreases and its acid strength increases. The increase in the acid strength occurs up to a Si/Al mol ratio of nearly 10 for which all aluminiums can be considered as isolated [32].

Due to the fact that for the target reaction two compounds with different polarities are involved (HMF is more polar than OBMF) and water is also formed as a reaction product, we have studied the effect of catalyst polarity on the observed catalytic activity. By doing that, one can expect to find an optimum in the adsorption properties that will favour the adsorption and desorption of reactant and products, respectively, and the observed catalyst activity. For testing this, the etherification of HMF was carried out in the presence of beta zeolites with different Si/Al ratios, which were prepared in fluoride medium in order to minimize the number of internal defects [21] (H-Al-Beta-F 12.5, 25, 50 and 100). Fig. 3 shows the existence of a maximum of activity for the sample having a Si/Al mol ratio of 50, which possesses lower concentration of acid sites than H-Al-Beta-F 12.5 (Table 1). These results show that a high concentration of acid sites does not guarantee a high catalytic

activity, but the adsorption properties of the catalyst should also be considered due to the different adsorption properties of HMF, OBMF and water. According to this, if the catalyst has an optimal hydrophobicity, then it can adsorb the reactant HMF but the concomitantly formed water can be easily desorbed, hence displacing the reaction towards the conversion into OBMF. The results from Fig. 3 show that a more hydrophobic zeolite with lower concentration of acid sites results in a more active catalyst. Nevertheless, one can also see that if the concentration of acid sites is still reduced (Si/Al mol ratio 100), a point is reached at which the catalytic activity is controlled by the small number of acid sites present.

3.3. Effect of water removal during the etherification of HMF

As was described before, beta zeolite with a higher Si/Al ratio (50), and consequently with lower polarity, was a better catalyst for a reaction, such as the etherification wherein water is produced, than other samples with a larger number of active sites, but which are more hydrophilic. This is not surprising, if one takes into account that for such a reaction, it should be thermodynamically and kinetically beneficial to decrease the water adsorption on the catalytic surface. Therefore, in this part of the work, we will study the influence on the reaction rate of operating within the presence of the water formed during the reaction, or by performing the reaction while water is continuously removed. In this second case and since HMF etherification into OBMF generates the concomitant formation of water, its removal from the reaction medium should improve the performance by shifting the equilibrium and by preventing deactivation of the catalyst by the adsorption of water on the active sites.

Since water and TFT are not miscible, while they form an azeotrope which distillates at 80 °C (90 mol% TFT), water can be removed from the reaction media by using an inverse Dean–Stark trap. Working under these conditions, different experiments were carried out with the most active and selective catalyst, i.e. Al-MCM-41 12.5. From the results presented in Table 4, we can see that in this case, it was possible to achieve full conversion with 97% selectivity to OBMF after 1-h reaction time. Clearly, this result is better than the one achieved without the Dean–Stark trap that requires 2 h to reach 99 mol% yield to OBMF (entry 5 in Table 3). Therefore, the removal of water during the reaction clearly favours the increase in catalytic activity.

On the basis of the remarkable improvement of the catalytic performance obtained as a result of water removal, it was thought to reduce the catalyst loading from 40 to 10 wt%. Under these con-
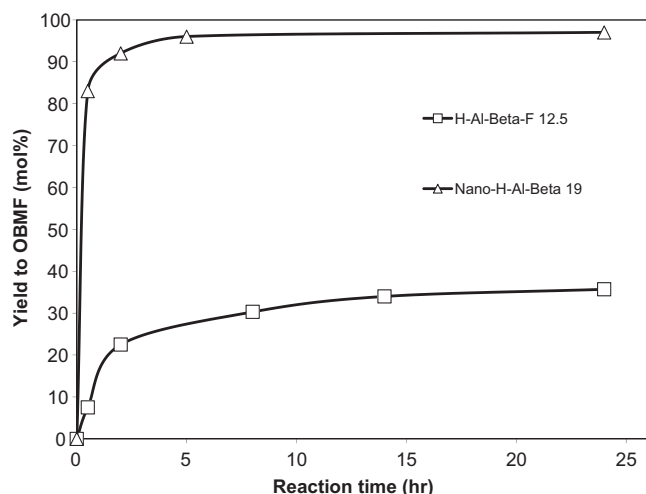

Fig. 2. Kinetics of the yield to OBMF (mol%) for two beta zeolites with different particle size (H-Al-Beta-F 12.5, regular size, and Nano-H-Al-Beta 19, nanocrystalline), in TFT, at 100 °C and 0.45 M HMF.
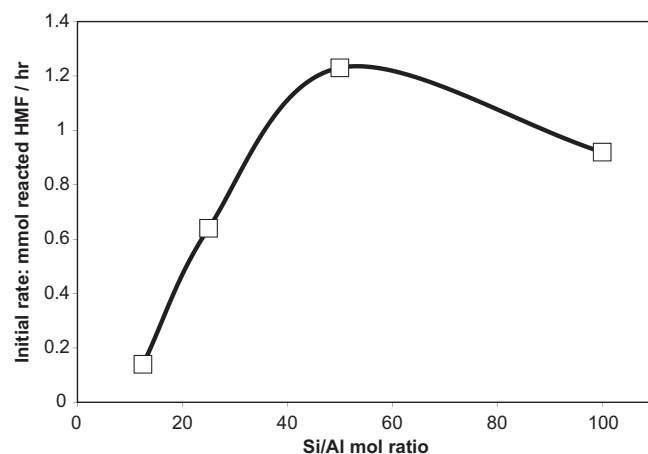

Fig. 3. Influence of the Si/Al mol ratio of different aluminium beta zeolites (H-Al-Beta-F 12.5, 25, 50 and 100) on the initial rate of conversion of HMF into OBMF.

Table 4
Effect of the removal of water generated in the etherification of HMF into OBMF with the optimal Brönsted acid catalysts at 100 °C, in TFT.[a]

Entry	Catalyst	Amount of catalyst (mg)	t (h)	Conversion (mol%)	Selectivity (mol%)
1	Al-MCM-41	125	1	98	>99
2	Al-MCM-41	30	1	66	98
			10	>99	97
3	Al-MCM-41[b]	30	21	56	>99
4	Al-MCM-41[c]	30	10	>99	97

[a] Reaction conditions: 315 mg HMF (2.5 mmol) in 14 mL TFT and 4 mL mQ water with the corresponding amount of catalyst were fed to a three-necked round-bottomed flask equipped with an inverse Dean–Stark trap (8 mL) to remove the water. The mixture was heated at its reflux temperature.
[b] Same as in entry 2 but without the inverse Dean–Stark trap.
[c] Same as in entry 2 but after calcination of the catalyst at 500 °C after its use in reaction.

ditions, (see entry 2, Table 4), 66 mol% yield to OBMF was obtained after 1 h, reaching 97 mol% after 10 h reaction. For comparison purposes, when the experiment was carried out without removing water (entry 3, Table 4), the yield of OBMF obtained was stabilized at 56 mol% after 21 h. As we anticipated previously, the catalyst Al-MCM-41 could be recovered after its use, and after calcination, it could be reused without any activity loss (entry 4, Table 4).

Therefore, taking into account the moderate reaction conditions, the inert and recoverable characteristics of the TFT solvent, as well as the possibility of operating in the presence of water or, even better, in absence of water, the results presented here indicate that ordered mesoporous aluminosilicates and tridimensional large pore zeolites with a certain hydrophobic character are catalysts of potential interest to synthesize OBMF from HMF obtained from glucose.

3.4. Synthesis of OBMF catalysed by solid Lewis acid catalysts

A series of beta zeolite and mesoporous catalysts containing no Brönsted but Lewis acid sites were prepared by introducing transition metal atoms in framework positions. We have presented previously that with the specific synthesis method reported [24–28], the metals occupy framework positions. With those materials, the etherification reaction was carried out at 100 °C with a catalyst loading equivalent to a HMF/Metal mol ratio of ca. 80. As can be observed (entries 1–4, Table 5), the Ta-Beta zeolite exhibited the highest initial rate among the materials prepared and, together with Sn-Beta, displayed the best yield of OBMF (ca. 69 and 78 mol%, respectively), while both Nb- and Zr-Beta gave much poorer results.

Acidity measurements of the Lewis acid catalysts are shown in Table 2. As can be seen there, the values of Lewis acidity are very close to each other. Nevertheless, their catalytic activity varies con-

Table 5
Etherification of HMF to OBMF in TFT with Lewis acid catalysts.[a]

Entry	Catalyst	Initial rate (mmol/h)	t (h)	Conversion (mol%)	Selectivity (mol%)
1	Sn-Beta	0.40	24	78	>99
2	Zr-Beta	0.13	24	35	>99
3	Nb-Beta	<0.01	24	39	>99
4	Ta-Beta	0.88	24	69	>99
5	Sn-MCM-41	0.66	4	84	>99
6	Zr-MCM-41	<0.01	24	<2	–

[a] Reaction conditions: 126 mg HMF (1.0 mmol) in 2.3 mL (TFT) with the corresponding amount of catalyst were fed to a three-necked round-bottomed flask. The mixture was heated at 100 °C. HMF/Metal mol ratio was maintained constant at 80 throughout all these tests.

siderably. This can be related to the distinct metal–substrate interaction for each metal site. Indeed, Boronat et al. [19b,19c] have shown that the catalytic activity is determined by the orientation of the d orbitals of the metal in the zeolite framework, the electronic interactions from the Lewis acid to the orbital of the base, as well as changes in the electronic levels of the active site caused by the latter interaction with the reactant molecule. Nevertheless, as can be observed in Fig. 4, all metal beta catalysts are less active than the corresponding Al-Beta. They also show fast deactivation, which could be attributed to micropore blocking as a result of the diffusion hindrance of the bulky OBMF. In fact, when the reaction was carried out with Sn-MCM-41 under the same conditions, the catalytic performance was improved achieving (entry 5, Table 5 and Fig. 4) high initial rate and high yield of OBMF in short reaction time. However, as can be seen in Fig. 4, Sn-MCM-41 also suffered a fast deactivation and reached a maximal conversion of 84 mol% after 4 h reaction time. This deactivation could be ascribed to a strong adsorption of the water and OBMF on the metal sites. The negative effect of product adsorption on the reaction rate in the case of metal-substituted molecular sieves was previously shown during the Baeyer–Villiger oxidation of ketones where the slow-down of the reaction was mainly due to the interaction of the Lewis acid sites with the carbonyl groups of the ester product [33]. In order to check if the same catalyst deactivation mechanism was working in our system, the etherification of HMF with Sn-MCM-41 was carried out in the presence of a given amount of furfural which will compete for adsorption on the Lewis acid sites through the interaction with the carbonyl group. The results in Fig. 5 confirm a decrease in the initial rate of reaction in the presence of furfural. It appears then that with the metalosilicate materials, when a certain concentration of OBMF is reached, the product competes with the HMF for adsorption on the Lewis site, hence decreasing strongly the reaction rate.

With regard to the catalyst stability, we could observe that the reuse of Sn-MCM-41 after successive washings with solvents gave very poor conversion. However, calcination at 500 °C after use resulted in complete recovery of its catalytic activity (Fig. 6).

3.5. Influence of solvent

Since toluene and TFT showed important differences in terms of activity and selectivity, we have used other similar solvents to per-
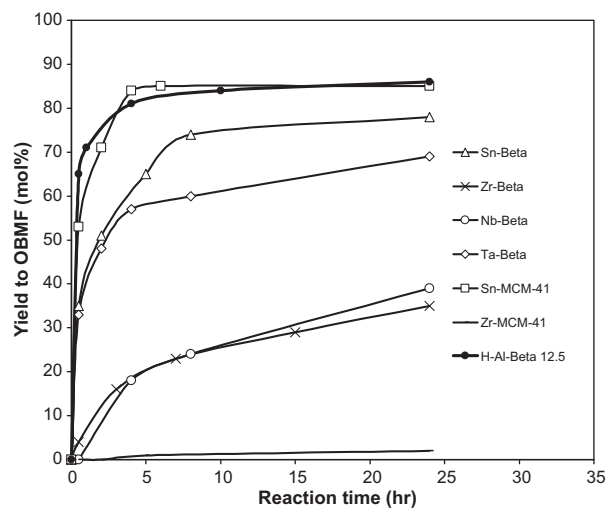

Fig. 4. Kinetics of the yield to OBMF (mol%) obtained for different solid Lewis acid catalysts compared with H-Al-Beta 12.5, in TFT, at 100 °C, 0.45 M HMF and HMF/Metal mol ratio 80.
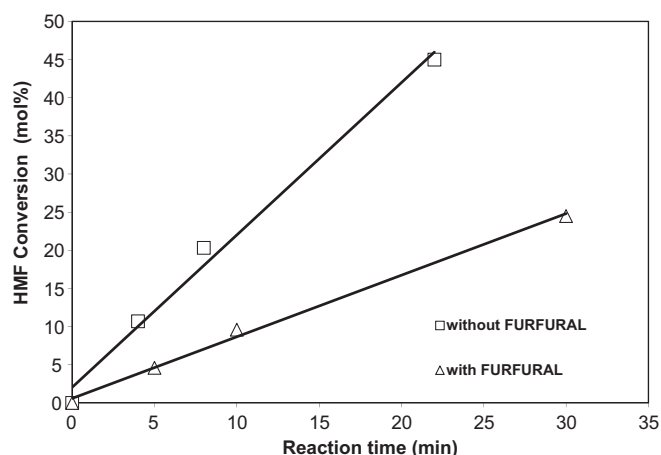
Fig. 5. Influence of furfural in the initial rate of the etherification of HMF into OBMF, at 100 °C, in TFT, using Sn-MCM-41 as catalyst, 0.45 M HMF and HMF/Metal mol ratio 160.
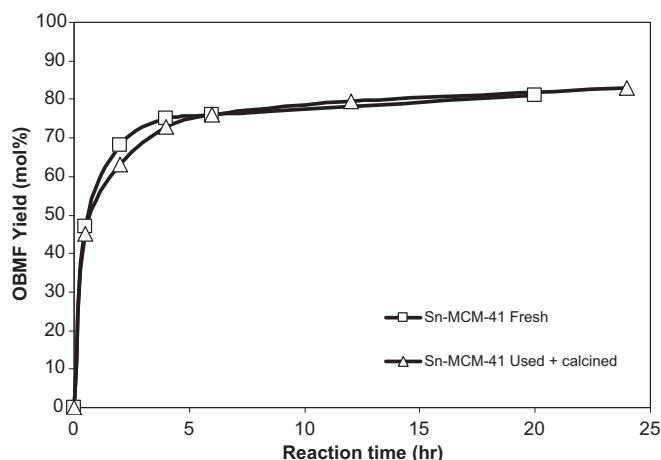

Fig. 6. Kinetics of the yield to OBMF (mol%) obtained with fresh and used (followed by calcination) Sn-MCM-41 catalysts, in TFT, at 100 °C, 0.45 M HMF and HMF/Metal mol ratio 160.

Table 6
Effect of solvent in the etherification of HMF into OBMF with Sn-MCM-41.[a]

Entry	Solvent (temperature, °C)	Initial rate (mmol/h)	t (h)	Conversion (mol%)	Selectivity (mol%)
1	Toluene (100)	0.90	8	75	91
2	Mesithylene (100)	1.42	3	93	33
3	Durene (100)	1.32	3	87	75
4	Durene (120)	1.62	3	93	56
5	4-Chlorotoluene (100)	0.70	9	84	>99
6	4-Chlorotoluene (120)	0.84	9	90	>99
7	Water	–	24	0	–
8	MIBK	–	24	0	–
9	Acetonitrile	–	24	0	–

[a] Reaction conditions: 126 mg HMF (1.0 mmol) in 2.3 mL solvent, with 50 mg Sn-MCM-41 catalyst were fed to a three-necked round-bottomed flask at each corresponding temperature.

Table 7
Effect of solvent in the etherification of HMF into OBMF with Al-MCM-41[a].

Entry	Solvent	Initial rate (mmol/h)	t (h)	Conversion (mol%)	Selectivity (mol%)
1	Toluene	1.72	2	99	20
2	Mesithylene	1.75	2	99	15
3	Durene	1.66	2	87	65
5	4-Chlorotoluene	1.4	2	95	>99
7	Water	–	24	0	–
8	MIBK	–	24	0	–
9	Acetonitrile	–	24	0	–

[a] Reaction conditions at 100 °C: 126 mg HMF (1.0 mmol) in 2.3 mL solvent, with 50 mg Sn-MCM-41 catalyst were fed to a three-necked round-bottomed flask at each corresponding temperature.

showing >99% selectivity towards OBMF, the values of conversion were fairly comparable to those obtained in the presence of TFT, although longer reaction times were required with 4-chloro-toluene using the Lewis Sn-MCM-41 catalyst. Nevertheless, with the Lewis acid catalyst, if the reaction temperature is increased to 120 °C, high reaction rate and conversion up to 90 mol% (entry 6, Table 6) can be observed without a noticeable loss of selectivity. Thus, it seems that TFT together with 4-chlorotoluene allows reactant dissolution and displays the best performance (highest activity and selectivity) when Al-MCM-41 and Sn-MCM-41 catalysts are used. We can then conclude that solvents with a deactivated aromatic ring have adequate polarity and reaction refractiveness for alkylation to allow the process to proceed with excellent selectivity. In addition, when water, methylisobutylketone (MiBK) and acetonitrile were used as solvents (Tables 6 and 7), no conversion of HMF to OBMF was observed. Besides this, alcohols such as methanol and ethanol react with HMF to give the corresponding acetals.

4. Conclusions

We have shown that the etherification of HMF to OBMF can be performed with high conversion and selectivity using molecular sieves with Brönsted and Lewis acid sites. Among them, mesoporous materials (Al-MCM-41 and Sn-MCM-41) give a better performance than zeolites. This is attributed to the existence of diffusional constraints in the microporous materials. Particularly, Al-MCM-41 bearing Brönsted acid sites gives better results than a homogeneous acid catalyst, such as para-toluenesulphonic acid. The former has the further advantage that can be recovered and reused. On the other hand, Sn-MCM-41 bearing Lewis acid sites displays lower catalytic activity.

form the etherification reaction. We chose the most active Lewis and Bronsted acid catalysts observed previously (Al-MCM-41 and Sn-MCM-41) as shown in Tables 6 and 7.

It was presented earlier that when toluene (activated aromatic ring) was employed as a solvent with Brönsted solid acid catalyst, by-products were formed as a result of solvent alkylation with dehydration intermediates of HMF (entry 2, Table 3). However, in the case of Sn-MCM-41, the selectivity to OBMF in the presence of toluene was higher than with the corresponding aluminosilicate Brönsted acid catalyst (entry 1, Table 7). In order to see if the solvent alkylation could be avoided by means of hindering this side reaction, we carried out the reaction using mesithylene and durene, which contain, respectively, three and four methyl groups in the aromatic ring. As can be observed (entries 2–4, Table 6), neither mesithylene nor durene were suitable for the etherification, as a result of the increased activation of the ring given by the methyl groups in the aromatic solvent and the inexistence of any relevant molecular hindering. In the case of Al-MCM-41 Brönsted acid catalyst, selectivities to OBMF were considerably lower (entries 2 and 3, Table 7).

The more deactivated 4-chloro-toluene (entries 5–6, Table 6, and entry 4, Table 7), is more adequate solvent than toluene from the point of view of conversion and selectivity. Indeed, apart from

Though the etherification reaction studied here does not require high acidities, the adsorption properties of catalyst, i.e. surface polarity plays a very important role for the catalytic activity finally observed.

Additionally, TFT has been proven to be a suitable solvent to carry out this reaction, not only because of the high reaction selectivity, but also because of the excellent reactant solubility and easy recovery. The properties of this solvent allows to continuously remove the water formed by distillation, which results in yields of OBMF of 99% which are the highest ever presented.

Acknowledgments

References

[1] Z. Hui, A. Gandini, Eur. Polym. J. 28 (1992) 1461–1469.
[2] C. Moreau, M.N. Belgacem, A. Gandini, Top. Catal. 27 (2004) 11–30.
[3] R. Wen, F. Yu, X. Dong, Y. Miao, P. Zhou, Z. Lin, J. Zheng, H. Wang, L. Huang, D. Qing, CN 1456556, 2003.
[4] Merck Company, Inc., GB 887360, 1962.
[5] D.J. Cram, DE 2539324, 1976.
[6] D. Chundury, H.H. Szmant, Ind. Eng. Chem. Prod. Res. Dev. 20 (1981) 158–163.
[7] B.C. Shi, B.H. Davis, J. Catal. 157 (1995) 359–367.
[8] P. Berteau, S. Ceckiewicz, B. Delmon, Appl. Catal. 31 (1987) 361–383.
[9] F.M. Bautista, B. Delmon, Appl. Catal. A Gen. 130 (1995) 47–65.
[10] G.A. Olah, T. Shamma, G.K.S. Prakash, Catal. Lett. 46 (1997) 1–4.
[11] F.P. Heese, M.E. Dry, K.P. Moller, Catal. Today 49 (1999) 327–335.
[12] C. Park, M.A. Keane, J. Mol. Catal. A Chem. 166 (2001) 303–322.
[13] M. Hunger, T. Horvath, J. Weitkamp, Micropor. Mesopor. Mater. 22 (1998) 357–367.
[14] F. Collignon, R. Loenders, J.A. Martens, P.A. Jacobs, G. Poncelet, J. Catal. 182 (1999) 302–312.
[15] E. Collignon, M. Mariani, S. Moreno, M. Remy, G. Poncelet, J. Catal. 166 (1997) 53–66.
[16] M. Hunger, T. Horvath, Catal. Lett. 49 (1997) 95–100.
[17] S.H. Brown, US 5444168, 1995.
[18] I. Hoek, T.A. Nijhuis, A.I. Stankiewicz, J.A. Moulijn, Appl. Catal. A Gen. 266 (2004) 109–116.
[19] (a) A. Corma, M. Renz, Angew. Chem., Int. Ed. 46 (2007) 298–300;
(b) M. Boronat, A. Corma, M. Renz, G. Sastre, P.M. Viruela, Chem. Eur. J. 12 (2006) 7076–7077;
(c) M. Boronat, A. Corma, M. Renz, G. Sastre, P.M. Viruela, Chem. Eur. J. 11 (2005) 6905–6915.
[20] M.J. Climent, A. Corma, A. Velty, M. Susarte, J. Catal. 196 (2000) 345–351.
[21] M.A. Camblor, A. Corma, S. Valencia, J. Mater. Chem. 8 (1998) 2137–2145.
[22] M.A. Camblor, A. Corma, A. Mifsud, J. Pérez-Pariente, S. Valencia, Stud. Surf. Sci. Catal. 105 (1997) 341–348.
[23] J.S. Beck, C. Chu, I.D. Johnson, C.T. Kresge, M.E. Leonovicz, W.J. Roth, J.C. Vartuli, WO 11390, 1991.
[24] S. Valencia, A. Corma, US 5968473, 1999.
[25] Y. Zhu, G. Chuah, S. Jaenicke, J. Catal. 227 (2004) 1–10.
[26] A. Corma, F.X.Ll. Xamena, M. Renz, S. Valencia, C. Prestipino, J. Phys. Chem. C 113 (2009) 11306–11315.
[27] T.K. Das, K. Chaudhari, A.J. Chandwadkar, S. Sivasanker, J. Chem. Soc., Chem. Commun. 24 (1995) 2495–2496.
[28] M.A. Camblor, A. Corma, H. García, V. Semmer-Herlédan, S. Valencia, J. Catal. 177 (1998) 267–272.
[29] F. Fajula, E. Bourgeat-Lami, C. Zivkov, T. Des-Courieres, P. Anglerot, EP 0488867, 1991.
[30] K. Chaudhari, T.K. Das, P.R. Rajmohanan, K. Lazar, S. Sivasanker, A.J. Chandwadkar, J. Catal. 183 (1999) 281–291.
[31] C.A. Emeis, J. Catal. 141 (1993) 347–354.
[32] D. Barthomeuf, Mater. Chem. Phys. 17 (1987) 49–71.
[33] M. Renz, T. Blasco, A. Corma, V. Fornes, R. Jensen, L. Nemeth, Chem. Eur. J. 8 (2002) 4708–4717.